Design of an interferometric displacement sensor with picometer resolution for the Galileo-Galilei mission

Marco Pisani and Giovanni Mana
Istituto Nazionale di Ricerca Metrologica
INRIM
Torino, Italy
m.pisani@inrim.it, g.mana@inrim.it

Anna M. Nobili
Department of Physics "E. Fermi", University of Pisa
and Istituto Nazionale di Fisica Nucleare
Pisa, Italy
nobili@dm.unipi.it

***Abstract*—The Galileo-Galilei (GG) mission aims at testing the Weak Equivalence Principle. It requires the measurement of the differential displacement between two test masses with a resolution of 1 pm/√Hz at 1 Hz. An optical interferometer has been designed to the purpose. The principle and the preliminary design of the interferometer will be illustrated.**

Keywords—Laser interferometer,

I. INTRODUCTION

General Relativity stands on the experimental fact that all bodies fall in a gravitational field with the same acceleration regardless of their mass and composition. This is the Universality of Free Fall (UFF) or the Weak Equivalence Principle (WEP). GG will test UFF/WEP to 1 part in 10^{17}[1]. It will do it by measuring the fractional differential acceleration of two test masses of different composition in the gravitational field of Earth while orbiting around it at low altitude. GG will improve the best tests to date – currently at 10^{-13} sensitivity level [2-4] – by four orders of magnitude, deeply probing a totally unexplored physical domain. The improvement on the best drop tests with cold atoms [5-8] will be huge, by 10 orders of magnitude. An experimental evidence of a UFF/WEP violation would mean that either General Relativity is to be amended, or that a new force of nature is at play. It would amount to a scientific revolution, while a UFF/WEP confirmation at this sensitivity level would strongly constrain physical theories. There is no firm target as to the level at which violation should occur, but the higher the test sensitivity, the higher the chances to find new physics.

The GG sensor is sensitive to the differential accelerations acting in the plane perpendicular to the spin/symmetry axis (such as the violation signal). It is made of two concentric, hollow cylinders weakly coupled to form a balance whose beam is the symmetry and spin axis. The capacitance readout of the early GG design has now been replaced by a laser interferometry gauge, which is ideal for rejecting common mode effects, it is linear, works at any distance and allows a gap several times larger than cap sensors (thus reducing many error sources). This paper relates about the design of a laser interferometer to be used to measure the differential displacement of the two cylinders.

II. THE PRINCIPLE OF GG MEASUREMENT

In the GG design, the test cylinders, together with the whole spacecraft surrounding them, spin around the symmetry axis. The proof masses form a rotating 2D harmonic oscillator characterized by weak coupling and fast rotation, that is, above the natural coupling frequency. This ensures the self-centering of their centers of mass, no active centering being required. Thus, one-axis rotation (e.g. at 1 Hz) stabilizes the satellite while, at the same time, modulates the violation signal (see Fig. 1).

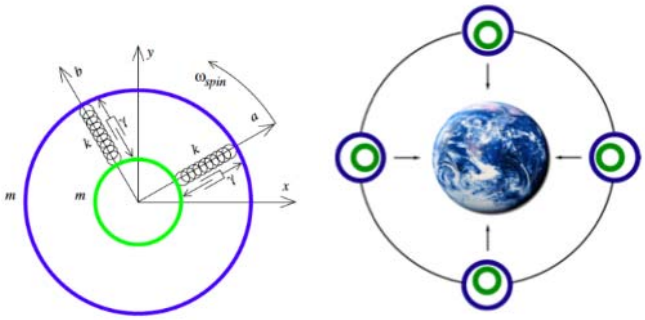

Fig. 1. A violation signal is shown to the right, as it affects the GG test cylinders in the orbit plane. The signal points to the Earth and in the simple case of a circular orbit has constant size. The sketch to the left shows the GG concentric cylinders coupled as a mechanical oscillator in 2D (the plane perpendicular to the spin/symmetry axis). The rotation up-converts the low frequency violation signal by a factor of 5800, from the orbital frequency to the spin frequency.

III. DESIGN OF THE NEW LASER GAUGE

GG uses nine laser gauges with sub-picometer performance to measure the relative displacements and, thus, the differential acceleration of the two test masses. Its conceptual layout is shown in Figs. 2 and 3, where three series of laser gauges are placed symmetrically at each end of the test masses and at the center.

978-1-4799-7569-3/15/$31.00 ©2015 IEEE

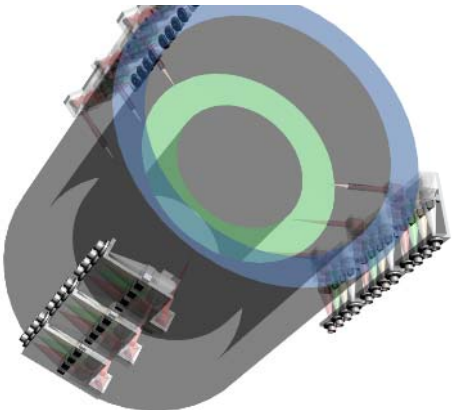

Fig. 2. A view of the nine laser gauges fixed to the PGB (Pico Gravity Box, an intermediate suspended stage, also of cylindrical shape, between the test masses and the spacecraft outer shell) aiming at the cylindrical test masses.

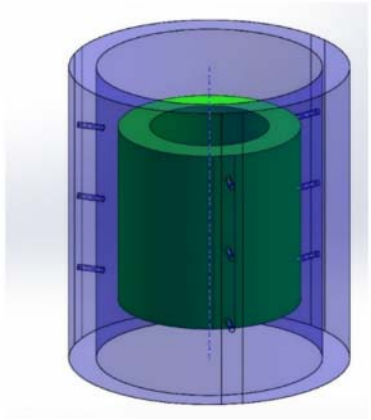

Fig. 3. Cylindrical test masses (10 kg each) with opto-mechanical machining to host the metrology system. The holes in the external cylinder allow the interferometer beam to measure the internal cylinder.

This layout allows the differential acceleration defined by four degrees of freedom (two translations and two tip/tilt) between the two cylinders to be measured with some redundancy. Systematic errors, such as uniform thermal expansions of the cylinders, are taken out among the nine symmetric laser gauges. The GG laser gauge (LG) is based on the common-path heterodyne interferometer originally developed for the SIM mission [9]. The LG is based on a heterodyne Michelson interferometer where the two arms are spatially separated (and recombined) by an arrangement of physical stops, iris and mirrors without using polarizing optics. The result is a quasi-complete cancellation of the typical polarization mixing induced nonlinearities. Picometer performance has been demonstrated at the laser sensor level and higher systems levels (Fig. 4). Similar performances have been demonstrated in alternative layouts realized by the authors of this paper in [10 and 11]. The concept of spatial separation of the interferometer arms to minimize non linearity effects is shown in Fig. 5. The interferometer is fed by two laser sources (red and blue in the sketch) and has two optical outputs (green in the sketch).

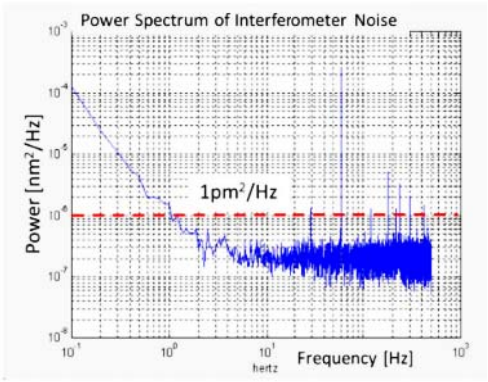

Fig. 4. Interferometer output obtained in laboratory with a breadboard of the spatially separated heterodyne interferometer realized as in [9]. The sub-picometer noise around 1 Hz is demonstrated.

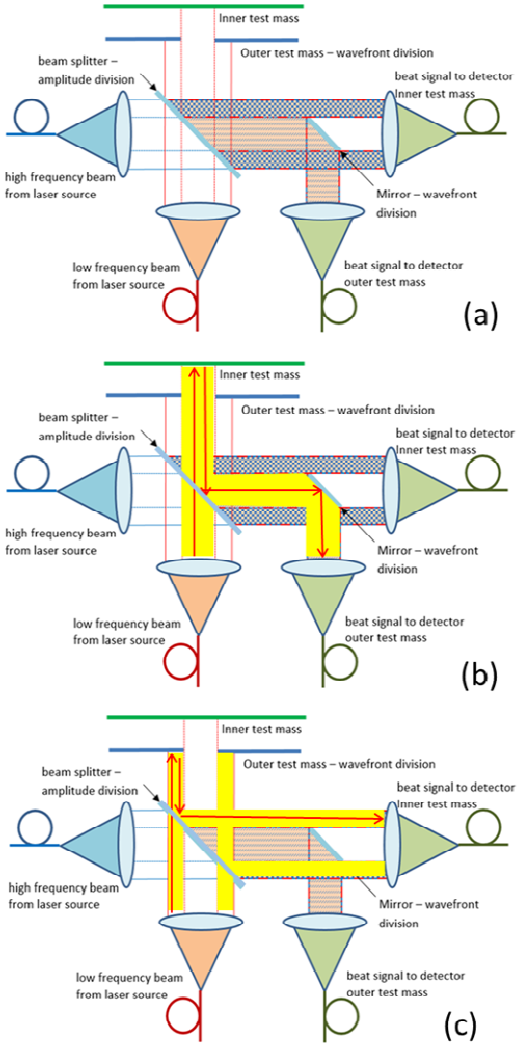

Fig. 5. Principle of the spatial separation of the interferometer arms to minimize non linearity effects in the laser gauge. a) a simplified schematic of the LG set-up as described in the text. b) path of the portion of the laser which goes towards the inner mass through a hole in the external mass, is reflected back, is redirected to the right side by the partially reflected mirror and finally is redirected towards one of the two detector lenses by a small mirror. The dimension of the mirror is such

that only the right part of the beam is «seen» by the detector. c) path of the beam going towards the external mass behaving as a ring shaped mirror, reflected back, redirected to the right side and finally passing over the small mirror now acting as a circular stop so that only the right part of the beam is collected by the lens.

The four laser lines are fiber coupled via collimating lenses (light blue in the sketch). The "red" laser source having frequency ν_1 is sent towards the test masses here represented as flat mirrors. The outer mass (blue line) has a hole that allows part of the beam to reach the inner mass (green line). Both mirrors reflect back the laser light to the beam splitter, which has experienced two different optical paths. The same beam splitter is illuminated by the "blue" laser source having frequency ν_2; here, the two laser beams interfere and generate an heterodyne signal at the frequency $\Delta\nu = \nu_2 - \nu_1$. The central part of the superposed beams delivers information about the inner mass position, the external part about the outer mass position. The two parts are eventually separated by a mirror so that they are sent by two different fibers to photo-detectors. The phase difference between the two heterodyne signals is measured with a phase meter. The differential displacement between the two test masses is then obtained by multiplying measured phase difference by $\pi/2$ times the laser wavelength. For displacements larger than $\pi/2$, the phase meter tracks integer counts.

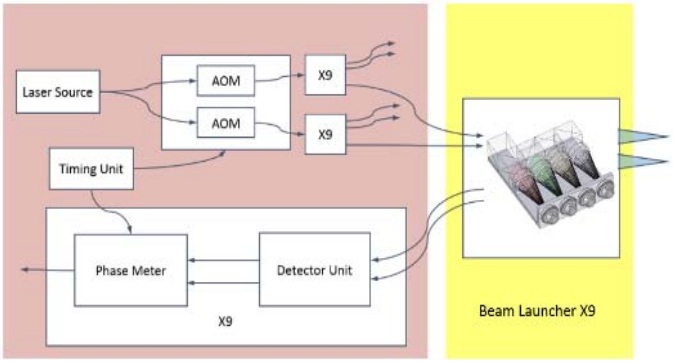

Fig. 6. schematic diagram of the opto-electronic set-up of the laser gauge.

A schematic diagram of the GG laser metrology system is shown in Fig. 6. The laser source is a continuous-wave non-planar ring-cavity oscillator (NPRO) with wavelength λ = 1.064 μm. The laser beam is split into two parts and undergoes differential frequency shift with the use of two acousto-optic modulators (AOMs) to generate ν_2 and ν_1. One laser frequency is used as the measurement beam, the other as the common local oscillator. Optical fiber couplers split the laser beams into nine parts to feed the nine laser gauges mounted around the test masses. The interferometer's beam launchers send the measurement beams to interrogate the outer and inner test masses. The power of the laser beams reflected on the test masses is kept as low as 1 μW in order to have a negligible effect due to the radiation pressure on the displacement of the masses. This power level, on the other hand, is high enough to guarantee the S/N level to the interferometric signal.

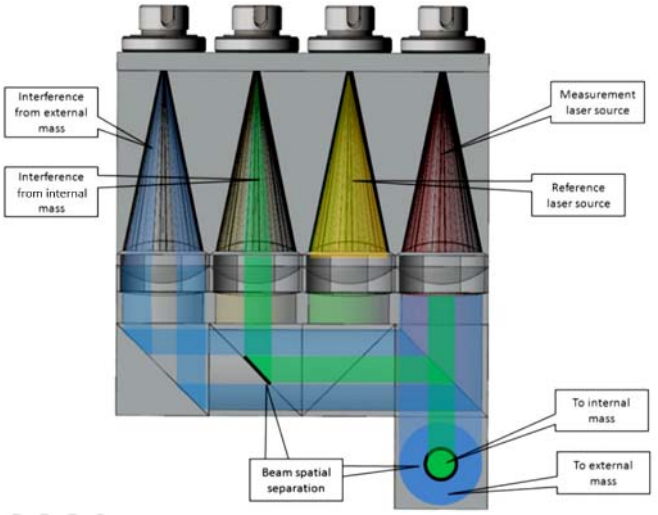

Fig. 7. Possible realization of the beam launcher (BL) fixed on the PGB (not visible) and aiming at the test masses. The BL assembly consists in four fibers (two inputs and two outputs) plus collimating lenses, as depicted in Fig. 5. No electronics is present on the BL assembly. The collimated laser beams are folded, split and combined by means of optical prisms.

The detail of a possible realization of the beam launcher and separation scheme is shown in Fig. 7. A scheme of the reflectors system (CCR) based on a split corner cube is shown in Fig. 8: a CCR with truncated vertex is embedded into the outer mass and retroreflects the external part of the laser beam. The central part of the laser beam passes through the polished surfaces of the truncated CCR and is reflected back by a smaller CCR embedded in the inner mass.

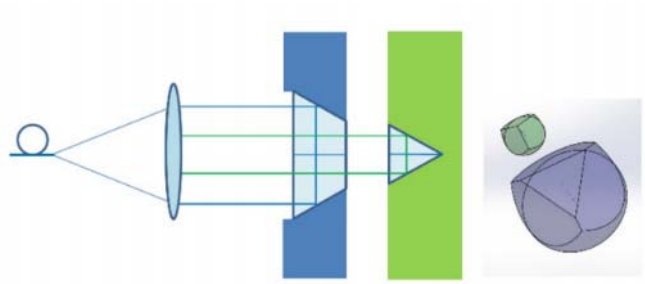

Fig. 8. Conceptual schematic of the possible launch optics for the laser gauge based on split corner-cube-retro-reflectors. A 3D representation of the two CCR is shown at the right.

IV. The Diffraction Issue

As explained in the previous chapter, the main error source in heterodyne interferometers is the cross-talk between the two optical paths that causes nonlinearities in the displacement vs phase function. In the proposed interferometer the beam separation is based on physical separation between two concentric optical paths. A simplified sketch is represented in Fig 9. In a practical realization, because of the limited dimensions of the optical head, the apertures and stops that implement the spatial separation will unavoidably cause diffraction. That means that part of the rays are deflected from

their straight path, thus going in the "wrong" direction. In other words, part of the signal that should go onto one detector, in fact, goes onto the other one (see Fig. 10). Roughly speaking, the proportion of the mixing effect (ratio between the unwanted and the wanted signal) generate proportional nonlinearity. The displacement error caused by diffraction is a fraction of the maximum displacement error given by the ratio of the test masses relative displacement over $\lambda/4$: the smaller the relative displacement of the masses, the smaller the effect of the diffraction error on the measured displacement. In GG, with 1 nm separation between the test masses, nonlinearities to the level of 0.01% would give 0.2 pm displacement error.

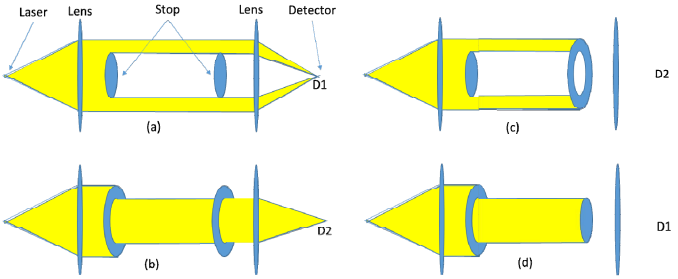

Fig. 9. Simplified representation of the measurement beams in the laser gauge. For the sake of clarity, the mass reflectors are represented in their own function as stop for a portion of the beam (first stop starting from the left). The beam is represented in a straight path from the fiber laser source (left), to the fiber detector (right). a) path of the laser reflected on the external mass reaching the detector D1. b) path of the laser reflected on the internal mass reaching detector D2. c) path of the laser reflected on the external mass stopped to prevent reaching detector D1. d) path of the laser reflected by the internal mass stopped to prevent reaching

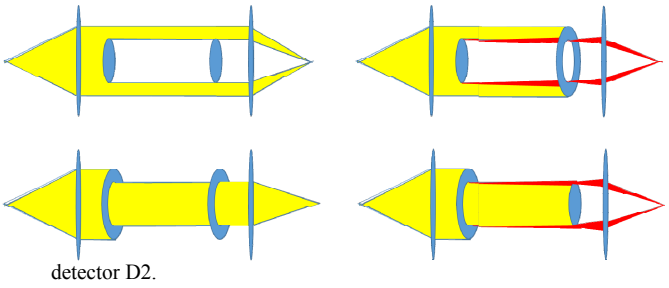

Fig. 10. Effect of the diffraction on the laser beam paths. Whenever the laser beam is truncated by a stop, diffraction occurs (red paths). This effect causes part of the beam to deviate off the right path and eventually reach the «wrong» detector. In other words in a real implementation the stops are not able to completely cancel the undesired signal

In order to evaluate the feasibility of a miniaturized optical head keeping the diffraction effect below the maximum allowed level, we have carried out numerical simulations as well as a preliminary experiment. The simple diffraction experiment (shown in Fig. 11) is based on a red laser source (633 nm) and makes use of irises and stops of the size foreseen for the GG-LG, scaled for the wavelength factor between 633 nm/1064 nm. The diffraction patterns are recorded by a high dynamic CCD sensor and the profiles are compared with the numerical simulation. The results of the experiment are shown in Figs. 12 to 14.

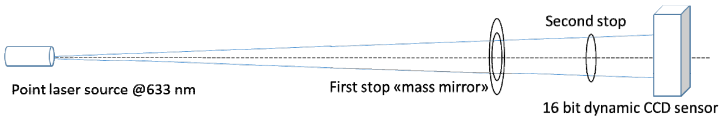

Fig. 11. experimental set-up for the evaluation of the diffraction effect. The first stop represent the "mass mirror" and can be an aperture (simulating the internal mass) or a stop (simulating the external mass). The second stop represents the mirror used to redirect the beam towards the detectors. Different stop and iris diameters have been used. The diameter size and the distance between the stops and the detector are scaled to take in account the difference between the simulator wavelength (633 nm) and the laser gauge wavelength (1064 nm).

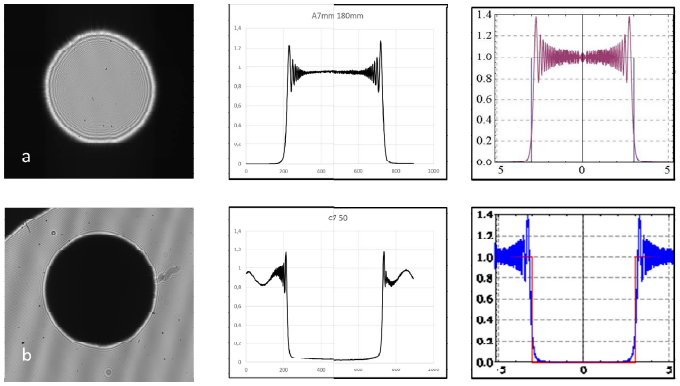

Fig. 12. Diffraction patterns and diffraction profiles. a) a 7 mm iris placed along the laser path selects the central part of the beam (representing the inner mass mirror). Diffraction distortion near the circumference is evident. The curve at the center is the normalized intensity profile along the diameter. The curve at the right side is a numerical simulation obtained with similar geomatrical configuration. b) The iris is removed and a 7 mm circular stop is placed close to the camera.

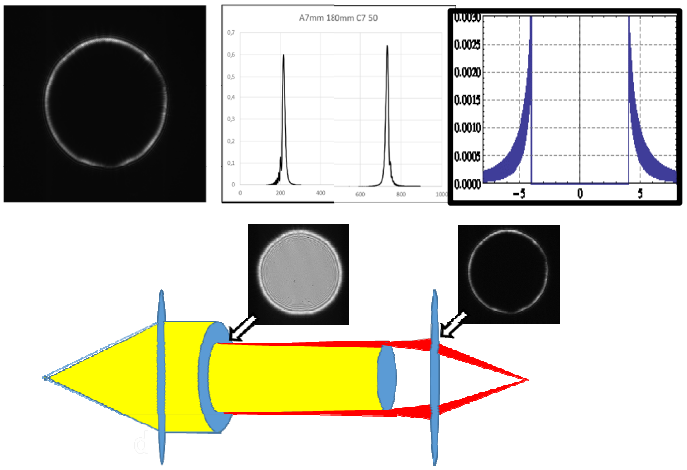

Fig. 13. Effect of the combination of ris and stop (simulator of the internal mass signal). The two objects of figure 12 are now on the beam, simulating one of the configurations of fig 10. A residual undesired ring is visible. The residual power is close to 1 % of the overall signal. A similar result is obtained with the numerical simulation at the up right side.

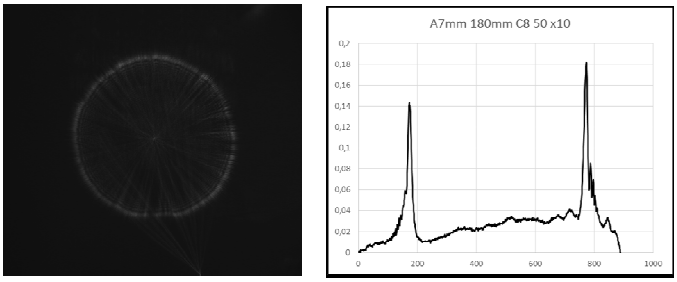

Fig. 14. Minimization of the spurious radiation. In order to reduce the spurious signal a 8 mm stop is used in place of the 7 mm one. The residual diffracted power is greatly reduced. Note that the image and the intensity profile are on x10 scale with respect to figure 13. The ratio between the residual and the wanted signal is now close to 10-4.

Both experimental and numerical results shown in figures 12 and 13 demonstrate that by using iris and stop of the same size a residual diffraction effect (ratio between the spurious and wanted signal) of the order of 1% is obtained. It is easy to demonstrate that by using a slightly larger stop the effect can be reduced down to 0.01% (see Fig. 14). That means that a separation of the two measurement channels to the required level can be easily obtained with a proper sizing of the apertures with a minimum effect on the intensity of the overall signal.

V. CONCLUSIONS

GG requires a metrology system to measure the differential displacement between the test masses with a resolution of 1 pm/√Hz at the spin frequency of 1 Hz to which the target signal is up-converted from the low orbital frequency of 1.7×10^{-4} Hz. It is well established that a readout based on laser interferometry can perform better than capacitance sensors. The laser interferometers envisaged for GG exploit spatial separation between the measurement arms in order to reduce nonlinearities to the required level. A preliminary experiment has demonstrated the feasibility of the reduction of the diffraction effect to the required 0.01%.

A breadboard of the laser gauge will be realized: a prototype of the beam launcher will be built and tested against a split corner-cube target in a vibration-controlled environment and in vacuum in order to test the performances at the real scale and to optimize the optoelectronic set up. The breadboard will be realized making use of standard components (laser, detectors optical elements etc.).

REFERENCES

[1] A.M. Nobili et al., Class. Quantum Grav. 29, 184011 (2012)

[2] S. Schlamminger et. al., Phys. Rev. Lett. 100, 041101 (2008)

[3] J. Mueller, F. Homan & L. Biskupek, Class. Quantum Grav. 29, 184006 (2012)

[4] J. G. Williams, S. G. Turyshev & D. H. Boggs, Class. Quantum Grav. 29, 184004 (2012)

[5] S. Fray et. al., Phys. Rev. Lett. 93, 240404 (2004)

[6] A. Bonnin,. et. Al., Phys. Rev. A 88, 043615 (5pp) (2013)

[7] D. Schlippert et. al., Phys. Rev. Lett. 112, 203002 (2014)

[8] M. G. Tarallo et. al., Phys. Rev. Lett. 113, 023005 (2014)

[9] M. Shao "SIM: the space interferometry mission", Proc. SPIE 3350, Astronomical Interferometry, 536 (1998); doi:10.1117/12.317092

[10] M. Pisani et al., Metrologia 49 455 (2012); doi:10.1088/0026-1394/49/4/455

[11] G. Cavagnero et al., Rev. Sci. Instrum. 76, 053106 (2005); doi:10.1063/1.189948